

# Quasi-epitaxy of a Tris(thieno)hexaazatriphenylene Derivative Adsorbed on Ag(110): Structural and Electronic Properties Probed by Scanning Tunneling Microscopy

Eric Salomon,<sup>\*,†</sup> Qing Zhang,<sup>‡</sup> Stephen Barlow,<sup>‡</sup> Seth R. Marder,<sup>‡</sup> and Antoine Kahn<sup>†</sup>

Department of Electrical Engineering, Princeton University, Princeton, New Jersey 08544, and School of Chemistry and Biochemistry and Center for Organic Photonics and Electronics, Georgia Institute of Technology, Atlanta, Georgia 30332-0400

Received: January 29, 2008; Revised Manuscript Received: April 7, 2008

Scanning tunneling microscopy is used to study the structure of monolayers of tris{2,5-bis(3,5-bis-trifluoromethyl-phenyl)-thieno}[3,4-*b,h,n*]-1,4,5,8,9,12-hexaaza-triphenylene adsorbed on a clean Ag(110) single-crystal surface. The molecules adsorb flat on the surface, forming two-dimensional islands within which intermolecular interactions constrain the molecules to form rows of molecular pairs. The balance between intermolecular and molecule–substrate interactions leads to two specific orientations of these rows at  $+11^\circ$  and  $-11^\circ$  from the [001] direction of the Ag(110) surface. A comparison between observed and calculated local densities of states shows an antiparallel azimuthal orientation of the molecules within the closely associated pairs. The structure of the full monolayer shows that the intermolecular interaction overcomes the interaction with the substrate, resulting in a reorientation of the rows along various directions.

## Introduction

One of the factors that limit the efficiency of organic devices is poor carrier mobility and low conductivity in organic materials. This challenge can be partly addressed by using molecular materials with delocalized  $\pi$ -orbitals, which form columnar structures of molecules with strongly overlapping  $\pi$ -electron systems. Typical applications of such molecular systems are in organic field effect transistors (OFETs), where molecular alignment along the channel is an asset for enhancing carrier mobility. For this reason, discotic materials appear to be an interesting class of candidates for application in organic electronics.<sup>1–4</sup> Among these materials, triphenylene and hexaazatriphenylene derivatives are particularly promising.<sup>5–8</sup> Moreover, it has been demonstrated that some of these compounds can be n-doped to alter the electron injection and transport properties of the film,<sup>8,9</sup> a property that could considerably enhance the performance of OFETs.

To date, several scanning tunneling microscopy (STM) and photoemission spectroscopy studies have been performed on molecular materials of this type.<sup>9–14</sup> However, most of these studies were performed on molecules adsorbed on “nonreactive” substrates, such as highly oriented pyrolytic graphite or crystalline gold (Au), with which molecules were expected to interact relatively weakly. Ha et al. recently examined via STM the growth of tris{2,5-bis(3,5-bis-trifluoromethyl-phenyl)-thieno}[3,4-*b,h,n*]-1,4,5,8,9,12-hexaazatriphenylene (THAP) (Figure 1a) on Au(111), and demonstrated the quasi-epitaxy of four molecular monolayer films of this compound.<sup>13</sup>

We also investigated the deposition of THAP on somewhat more reactive substrates, amorphous and crystalline silver (Ag), by means of photoemission spectroscopy,<sup>14</sup> and demonstrated a stronger chemical interaction than that found with Au, as evidenced by charge transfer from the metal surface to the first

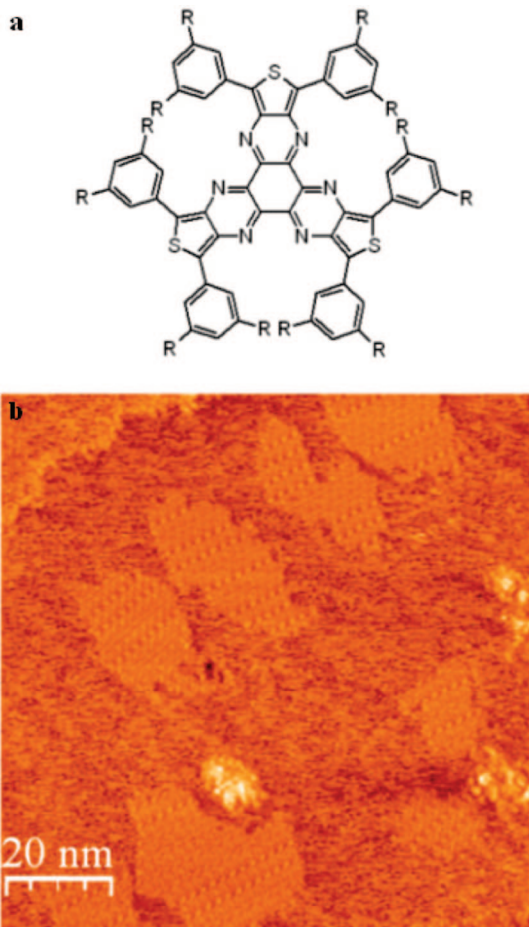


**Figure 1.** (a) Chemical structure of the THAP molecule; R stands for a trifluoromethyl group ( $-\text{CF}_3$ ). (b) STM images of a submonolayer coverage of THAP on Ag(110): 100 nm  $\times$  100 nm,  $V = -1.8$  V (filled states),  $I_t = 0.33$  nA.

molecular plane. In light of this work, here we study the structural aspect of the adsorption of THAP on a clean Ag(110)

\* Corresponding author. Phone: +1-609-258-3582. Fax: +1-609-258-6279. E-mail: esalomon@princeton.edu.

<sup>†</sup> Princeton University.

<sup>‡</sup> Georgia Institute of Technology.

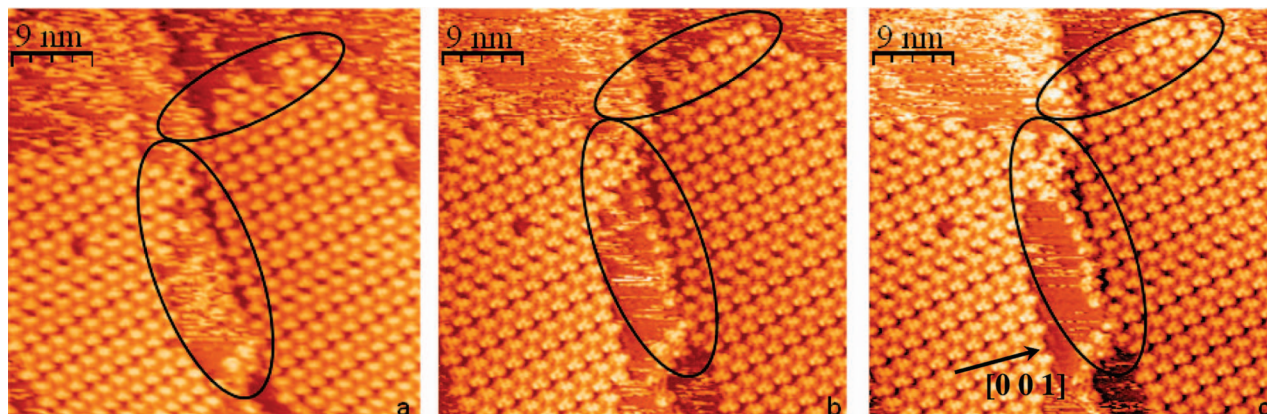


**Figure 2.** Time-series images of the same scanned area.  $45 \text{ nm} \times 45 \text{ nm}$ ,  $V = -1.2 \text{ V}$  (filled states),  $I_t = 0.24 \text{ nA}$ .

surface via STM. Of specific interest is the balance between molecule–substrate and molecule–molecule interaction. In that regard, the recent STM investigation of the growth of up to four quasi-epitaxial layers of THAP on Au(111) showed continuity of the structure from interface to surface,<sup>13</sup> suggesting predominance of intermolecular interaction over substrate-imposed molecular arrangement.

We show here that, on Ag(110), the THAP molecules organize in pairs and form two-dimensional islands consisting of rows. A comparison between the density of states observed by STM and the calculated density functional theory frontier orbitals<sup>8</sup> leads to the conclusion that each pair is composed of two molecules azimuthally oriented in opposite directions. We suggest that the molecules within each pair are linked to each other via  $\text{C}-\text{F}\cdots\text{H}-\text{C}$  bonds. Interestingly, at submonolayer coverage, the coupling between the molecules and the substrate induces a specific orientation of the rows along two specific directions. At full monolayer coverage, the molecular monolayer consists of numerous adjacent islands and the rows are oriented in various directions. It is suggested that substantial repulsive interisland forces, which overcome the molecule–substrate interaction, lead to a reorientation of the islands.

The molecular layers were deposited on a single-crystal Ag(110) purchased from Mateck. The preparation of the metallic surface, carried out in an ultrahigh vacuum (UHV) preparation chamber (base pressure of  $6 \times 10^{-11}$  Torr), consisted of several cycles of Ar-ion sputtering (500 or 1000 eV) and annealing (690 K). This procedure produced a clean and well-ordered metallic surface exhibiting a rectangular ( $1 \times 1$ ) unit cell. Low energy electron diffraction (LEED), also available in the preparation chamber, was used to verify long-range order on the metallic surface. THAP was synthesized and purified as previously described<sup>8</sup> and was placed in a quartz crucible in the preparation chamber. The molecules were deposited on the clean Ag(110) substrate by thermal evaporation ( $\sim 480 \text{ K}$ ) at a rate of  $0.3\text{--}0.5 \text{ \AA/min}$ . Evaporation rate and nominal film thickness were estimated using a calibrated quartz crystal microbalance. During deposition, the substrate was held at room temperature. The STM measurements were performed under UHV conditions (base pressure of  $4 \times 10^{-11}$  Torr) using a commercial Omicron room-temperature STM in an analysis chamber connected to the film preparation chamber. Images were recorded in constant current topographic mode and processed with the WSxM software.<sup>15</sup>

### Submonolayer Coverage

STM images of a nominal  $3 \text{ \AA}$  THAP layer deposited on Ag(110) show submonolayer coverage of the substrate with

molecules forming structurally ordered islands (Figure 1b). Images show that the adsorbed THAP molecules lie flat on the surface, as expected from numerous previous observations of the configuration of approximately planar molecules on metal surfaces. Typical island dimensions are  $20 \pm 10 \text{ nm} \times 15 \pm 10 \text{ nm}$ . Because the density of these islands is relatively small, and the scattering strength of the carbon-based molecules significantly weaker than that of Ag, no molecular superlattice pattern is seen at this coverage via LEED. The STM image also shows brighter protrusions that are attributed to molecular aggregates of disordered molecules.

At submonolayer coverage, a significant portion of the molecules is seen to diffuse over the surface, causing the observed horizontal bright stripes in the STM micrographs. This molecular diffusion is clearly demonstrated in a series of images taken consecutively 15 min apart and presented in Figure 2.

As can be seen in the encircled areas, molecules move on the surface and diffuse to the edges of both the Ag terraces and the molecular islands. As a result, the size of each island grows with time. The STM images reveal that after 72 h, the molecular islands are approximately double in area. The image also contains fewer horizontal stripes caused by molecular motion and larger areas of clean substrate.

The molecular-resolution images presented above and in Figure 3a and b show that the THAP islands consist of ordered rows of molecular pairs. On the figure each row is separated from another by a black line. One row is approximately  $41 \text{ \AA}$  wide, and the periodicity of the molecular pairs along a row is  $22 \text{ \AA}$ . This distance coincides with the average measured “diameter” of the THAP molecule ( $\sim 21 \text{ \AA}$ ).<sup>13</sup> The unit cell of the molecular lattice is a parallelogram ( $a = 22 \text{ \AA}$ ,  $b = 41 \text{ \AA}$ ,  $\alpha = 92^\circ$ ), each corner of which is the center of a molecular pair. Each molecule appears as a three-pronged shape with three bright protrusions surrounded by a less intense ring. The average distance between two bright protrusions is  $9 \text{ \AA}$ . This value corresponds to previous measurements performed on 5,6,11,12,17,18-hexaazatrinaphthylene molecules and triphenylene-based architectures.<sup>10,12</sup> Along with previous STM studies of THAP on Au(111),<sup>13</sup> this suggests that the three bright lobes correspond to the core of the molecule.

To further support this claim, we compare the filled- and empty-states STM images with representations of the occupied and unoccupied frontier orbitals obtained by density-functional theory (DFT) B3LYP/6-31G calculations.<sup>8</sup> Two STM micrographs of the surface taken with the sample biased at  $-1.30$  and  $+1.30 \text{ V}$  are shown in Figure 3c and d, respectively. At negative bias, electrons tunnel from the sample to the tip and the recorded image represents the local density of occupied states. At positive bias, the image corresponds to the local



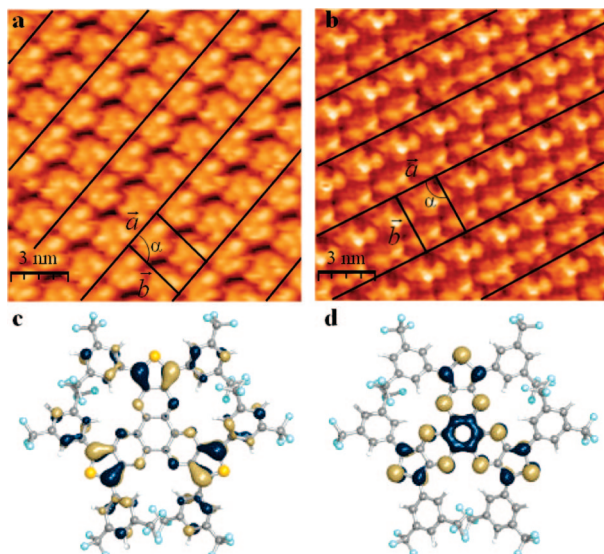


**Figure 3.** 15 nm  $\times$  15 nm STM images of the submonolayer recorded at (a)  $V = -1.3$  V (filled states) and (b)  $V = +1.3$  V (empty states). Representation of the frontier (c) HOMO and (d) LUMO of the THAP molecule derived from B3LYP/6-31G\*\* DFT calculations.

density of unoccupied states. Figure 3c and d displays the DFT highest occupied and lowest unoccupied molecular orbitals (HOMO and LUMO), respectively.

According to the chemical structure depicted in Figure 1a, we deduce for the image presented in Figure 3c that the observed density of occupied states is mainly localized on the sulfur-containing and nitrogen-containing rings of the molecule. This is in agreement with the DFT results presented in Figure 3c, which show that the local density of occupied states is localized mostly on the thieno ring of the molecule rather than on its center or periphery. Likewise, the local density of unoccupied states in Figure 3d follows the DFT LUMO shown in Figure 3d. The density of unoccupied states is principally localized on the central ring of the THAP core, extending somewhat onto the three arms of the tripod-like core of the THAP molecule.

A closer look at the molecular pairs reveals that they are composed of two THAP molecules azimuthally oriented in opposite directions. An antiparallel configuration of this sort has previously been observed for this compound as well as for several other tripod-core molecules.<sup>11,13,16–18</sup> This particular configuration may minimize steric hindrance and reduce surface energy. The packing is shown more clearly by superposition of the DFT structure of THAP<sup>8</sup> on the STM image so that each bright lobe in the image corresponds to an arm of the core of the molecule; this is shown in Figure 4a, with the corresponding unit cell of the molecular lattice shown in Figure 4b.

The latter suggests the possibility of  $\text{sp}^3\text{C}-\text{F}\cdots\text{H}-\text{sp}^2\text{C}$  interactions between the trifluoromethyl groups and phenyl hydrogen atoms on adjacent molecules. Interactions of this type are generally rather weak (for example, energies of ca. 4–7 kJ mol<sup>-1</sup> have been computationally estimated for  $\text{sp}^3\text{C}-\text{F}\cdots\text{H}-\text{sp}^2\text{C}$  interactions<sup>19</sup>), and it is a matter of some debate whether one should term them “hydrogen bonds”. However,  $\text{C}-\text{F}\cdots\text{H}-\text{C}$  interactions are a feature of many crystal structures of fluorine-containing organic compounds,<sup>20,21</sup> and  $\text{C}-\text{F}\cdots\text{H}-\text{C}$  as well as  $\text{B}-\text{F}\cdots\text{H}-\text{C}$  interactions have also been observed in STM studies, for example, of zinc 2,3,9,10,16,17,23,24-octafluorophthalocyanine on Au(111)<sup>22</sup> and of dioxaborine derivatives of highly ordered pyrolytic graphite,<sup>23</sup> respectively. Thus,  $\text{C}-\text{F}\cdots\text{H}-\text{C}$  interactions may contribute to the energetic stabilization of the antiparallel orientation of pairs.

An interesting point emerging from Figure 1b is that the rows of antiparallel pairs are oriented along two specific directions,  $\pm 11^\circ$  relative to the [001] direction of the Ag surface. The origin of these specific orientations is shown in Figure 5, where the molecular lattice is superimposed to the Ag surface lattice. When the shorter side of the THAP unit cell, that is, the direction of the molecular row, is oriented along these two directions, each corner of the molecular unit cell parallelogram coincides with the corner of the substrate lattice unit cell within an accuracy of  $\pm 1$  Å. In Figure 5, we arbitrarily chose to illustrate this point-in-line coincidence<sup>24</sup> geometry by placing the corners of the molecular unit cell on top of the Ag atoms lattice sites. According to the adsorption geometry, the first point-in-line coincidence site along the longer side would have been around 20 Å. However, in this direction, the molecules of the second pair would have overlapped those of the first pair, resulting in very strong repulsive intermolecular interactions. Therefore, to minimize the surface energy, the second pair adsorbed on the second point-in-line coincidence site along this direction, which is 40 Å apart from the first pair. This type of quasi-epitaxial growth suggests a substantial interaction between the molecules and specific atoms of the metallic substrate. This conclusion is certainly compatible with photoemission spectroscopy measurements previously performed on THAP on Ag(110),<sup>14</sup> which indicate that an electron charge transfer occurs at the interface between the metal and the THAP layer. The molecule–substrate interaction is stronger than in the case of THAP on Au,<sup>13</sup> for which several differently oriented domains can be seen on a terrace. For THAP on Ag, the molecular adsorption seems to be imposed by the delicate balance between intermolecular and molecule–substrate forces.

### Full Monolayer Coverage

The molecule–substrate interaction plays an important role as well in defining the structure of the full monolayer. Complete molecular monolayers of THAP on Au have been shown to cover the substrate surface homogeneously with large ordered domains.<sup>13</sup> In the case of Ag(110), however, the full monolayer consists of numerous adjacent islands (Figure 6). While intermolecular van der Waals forces dominate in the Au(111) case, a stronger molecule–substrate chemical interaction occurs in the Ag(110) case.<sup>14</sup> A similar phenomenon was already reported in the case of the adsorption of perylenetetracarboxylicdianhydride (PTCDA) on Ag and Au.<sup>25,26</sup>

Two images of full molecular monolayers are presented in Figure 6a and b. The former was obtained upon evaporation of THAP at a rate of 0.5 Å/min on a Ag sample, sputtered with a beam energy of 500 eV, presenting relatively small terraces (<70 nm wide), while the latter was obtained with an evaporation rate nearly one-half of the former ( $\sim 0.3$  Å/min) on a Ag sample, sputtered with a beam energy of 1000 eV, with larger terraces (>100 nm wide). In both cases, the total nominal thickness of the organic film was 9 Å. The average island size in the second case is significantly larger than that in the former, suggesting that the evaporation of the molecules at a lower deposition rate and on a surface presenting larger terraces allows more time for diffusion and formation of large ordered domains, thus reducing the number of grain boundaries.

As in the submonolayer case, the islands observed at full monolayer coverage consist of ordered molecular rows. However, several orientations of these rows are observed, in contrary to the submonolayer coverage case presented above where only two different orientations were observed. The origin of this reorientation of the rows remains unclear. Because of the

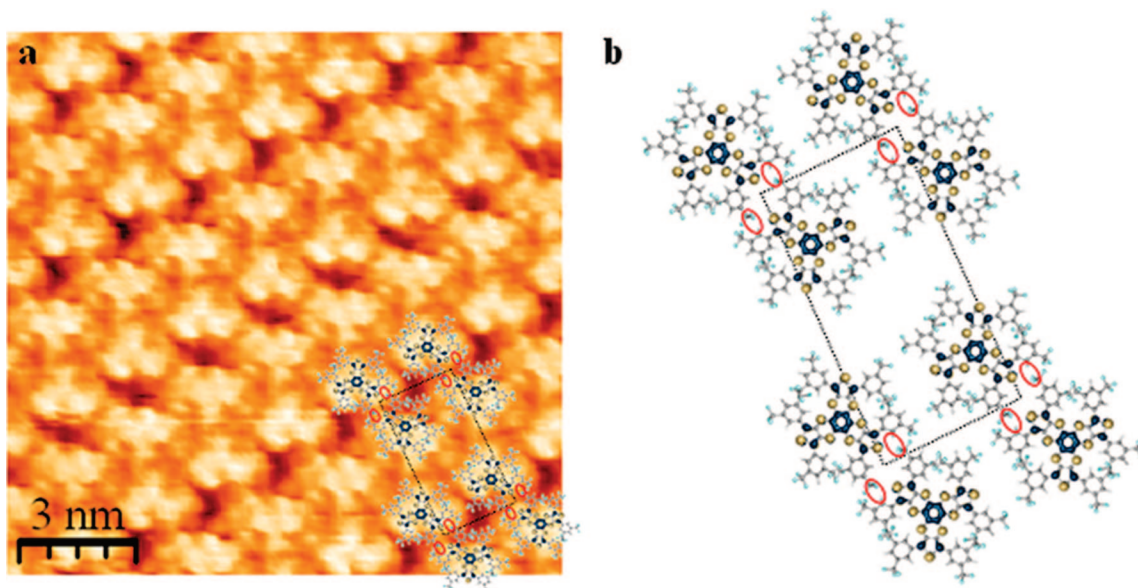


**Figure 4.** (a) Molecular-resolution view of the rows with representation of the unit cell (15 nm  $\times$  15 nm,  $V = -1.2$  V (filled states),  $I = 0.24$  nA). (b) Unit cell with representation of the C-F...H-C interaction.

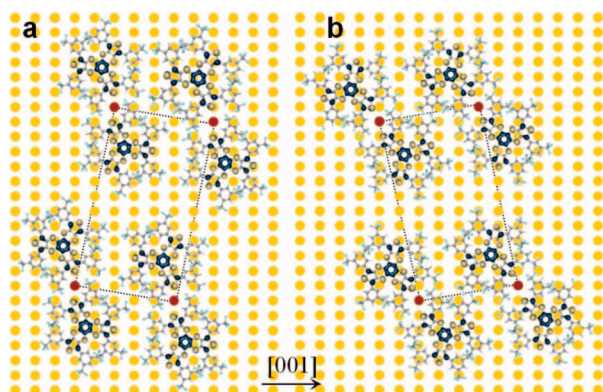


**Figure 5.** Schematic representation of the registry of the THAP molecular lattice with respect to the Ag(110) lattice, with specific orientations of the rows at  $-11^\circ$  (a) and  $+11^\circ$  (b).

predominant islanding growth mode of THAP on Ag and the strong interaction between molecule and substrate, the THAP islands remain rigidly in place and thus lead to a significant density of grain boundaries. Moreover, the large number of fluorine atoms at the periphery of each molecule may result in repulsive forces between neighboring islands. Therefore, when a new island nucleates next to another one, that is, when the size of the new island is small enough, these repulsive forces might overcome the molecule–substrate interaction and induce a reorientation of the rows and, as a result, minimize the total surface energy. In addition, because the monolayer obtained at lower deposition rate presents significantly fewer different orientations and larger islands (Figure 6b), the reorientation is presumably also related to the kinetics of adsorption.

In summary, the evaporation of THAP on Ag(110) results in the formation of two-dimensional molecular islands. Good agreement between the observed density of filled and empty states of the adsorbed molecule and the theoretical calculations of frontier orbitals shows that THAP organizes in pairs of molecules facing in opposite directions. This antiparallel configuration may be influenced by C-F...H-C interactions between two adjacent molecules. At submonolayer coverage, the molecule–substrate interaction results in the formation of islands consisting of rows of in-pair molecules oriented in two

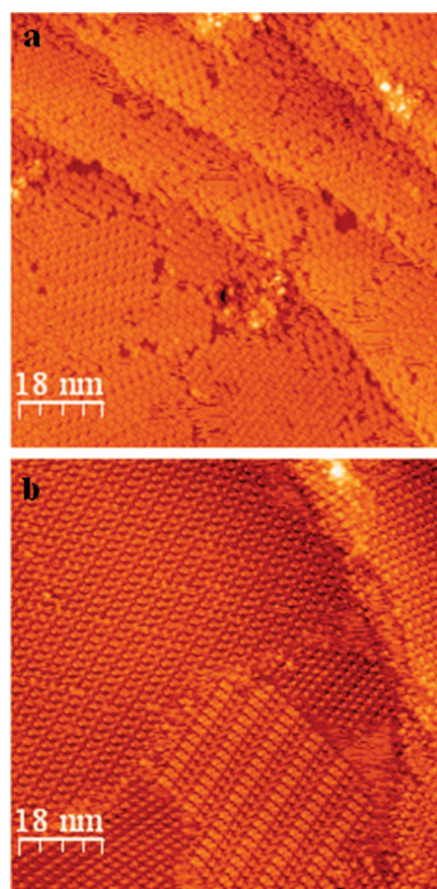


**Figure 6.** 90 nm  $\times$  90 nm STM images of the full monolayer coverage of THAP on Ag(110) ( $V = -1.2$  V (filled states),  $I_t = 0.2$  nA) obtained using a deposition rate of (a) 0.5 Å/min and (b) 0.3 Å/min.

specific directions. A reorientation of these rows is observed at higher molecular coverage. The basic mechanism behind this reorientation remains unclear, but the difference observed between the monolayers deposited at different rates suggests the importance of kinetics in the final molecular ordering. Also, at high coverage, the intermolecular interaction may overcome the coupling with the metallic surface and cause the reorienta-



tion. This illustrates that the order of the monolayer or of large molecular domains results from the competition between the kinetics of adsorption, the intermolecular forces, and the molecule–substrate interactions.

**Acknowledgment.** The Princeton group gratefully acknowledges support from the National Science Foundation (DMR-0705920) and the Princeton MRSEC of the National Science Foundation (DMR-0213706). Work at the Georgia Institute of Technology was supported by the National Science Foundation (CHE-0211419 and the STC Program under Agreement Number DMR-0120967), Lintec Corp., and the Office of Naval Research (N00014-04-1-0120).

## References and Notes

- (1) Adam, D.; Schuhmacher, P.; Simmerer, J.; Haussling, L.; Siemensmeyer, K.; Etzbach, K. H.; Ringsdorf, H.; Haarer, D. *Nature* **1994**, 371–141.
- (2) Boden, N.; Bushby, R. J.; Clements, J.; Movaghar, B.; Donovan, K. J.; Kreouzis, T. *Phys. Rev. B* **1995**, 52, 13274.
- (3) Van de Craats, A. M.; Warman, J. M. *Adv. Mater.* **2001**, 13, 130.
- (4) Bredas, J.-L.; Beljonne, D.; Coropceanu, V.; Cornil, J. *Chem. Rev.* **2004**, 104, 4971.
- (5) Van de Craats, A. M.; Siebbeles, L. D. A.; Bleyl, I.; Haarer, D.; Berlin, Y. A.; Zharikov, A. A.; Warman, J. M. *J. Phys. Chem. B* **1998**, 102, 9625.
- (6) Ke-Qing, Z.; Bi-Qin, W.; Ping, H.; Quan, L.; Liang-Fu, Z. *Chin. J. Chem.* **2005**, 23, 767.
- (7) Kumar, S. *Chem. Soc. Rev.* **2006**, 35, 83.
- (8) Barlow, S.; Zhang, Q.; Kaafarani, B. R.; Risko, C.; Amy, F.; Chan, C. K.; Domercq, B.; Starikova, Z. A.; Antipin, M. Y.; Timofeeva, T. V.; Kippelen, B.; Brédas, J. L.; Kahn, A.; Marder, S. R. *Chem.-Eur. J.* **2007**, 13, 3537.
- (9) Chan, C. K.; Amy, F.; Zhang, Q.; Barlow, S.; Marder, S. R.; Kahn, A. *Chem. Phys. Lett.* **2006**, 431, 67.
- (10) Palma, M.; Pace, G.; Roussel, O.; Geerts, Y.; Samorì, P. *Aust. J. Chem.* **2006**, 59, 376.
- (11) Palma, M.; Levin, J.; Lemaure, V.; Liscio, A.; Palermo, V.; Cornil, J.; Geerts, Y.; Lehmann, M.; Samorì, P. *Adv. Mater.* **2006**, 18, 3313.
- (12) Ha, S. D.; Kaafarani, B. R.; Barlow, S.; Marder, S. R.; Kahn, A. *J. Phys. Chem. C* **2007**, 11, 10493.
- (13) Ha, S. D.; Zhang, Q.; Barlow, S.; Marder, S. R.; Kahn, A. *Phys. Rev. B* **2008**, 77, 085433.
- (14) Salomon, E.; et al., to be submitted.
- (15) Horcas, I.; Fernandez, R.; Gomez-Rodriguez, G. M.; Colchero, J.; Gomez-Herrero, J.; Baro, A. M. *Rev. Sci. Instrum.* **2007**, 78, 013705.
- (16) Askadskaya, L.; Boeffel, C.; Rabe, J. P. *Ber. Bunsen-Ges. Phys. Chem.* **1993**, 97, 517.
- (17) Wu, P.; Zeng, Q.; Xu, S.; Wang, C.; Yin, S.; Bai, C.-L. *ChemPhysChem* **2001**, 2, 750.
- (18) Osipov, M. A.; Stelzer, J. *Phys. Rev. E* **2003**, 67, 061707.
- (19) Hunter, L.; Slawin, A. M. Z.; Kirsch, P.; O'Hagan, D. *Angew. Chem., Int. Ed.* **2006**, 46, 7887.
- (20) Howard, J. A. K.; Hoy, V. J.; O'Hagan, D.; Smith, G. T. *Tetrahedron* **1996**, 52, 12613.
- (21) Shimon, L.; Glusker, J. P. *Struct. Chem.* **1994**, 5, 383.
- (22) Oison, V.; Koudia, M.; Abel, M.; Porte, L. *Phys. Rev. B* **2007**, 75, 035428.
- (23) Zhang, X.; Yan, C.-J.; Pan, G.-B.; Zhang, R.-Q.; Wan, L.-J. *J. Phys. Chem. C* **2007**, 111, 13851.
- (24) Mannsfeld, S. C. B.; Fritz, T. *Phys. Rev. B* **2004**, 69, 075416.
- (25) Böhrringer, M.; Schneider, W.-D.; Berndt, R.; Glöckler, K.; Sokolowski, M.; Umbach, E. *Phys. Rev. B* **1998**, 57, 4081.
- (26) Schmitz-Hübsch, T.; Fritz, T.; Sellam, F.; Staub, R.; Leo, K. *Phys. Rev. B* **1997**, 55, 7972.

JP800858U